Available online at www.sciencedirect.com
ScienceDirect
Ceramics International 35 (2009) 1057–1062
CERAMICS INTERNATIONAL
www.elsevier.com/locate/ceramint

Electrical studies on A- and B-site-modified $Bi_4Ti_3O_{12}$ ceramic

N.V. Prasad [a,*], S. Narendra Babu [b], A. Siddeshwar [b], G. Prasad [b], G.S. Kumar [b]

[a] Department of Physics, PG Centre, P.B. Siddhartha College of Arts & Science, Vijayawada 520010, India
[b] Department of Physics, Osmania University, Hyderabad 500007, India

Received 24 October 2007; received in revised form 17 March 2008; accepted 24 April 2008
Available online 12 July 2008

Abstract

Pure and niobium-doped samarium bismuth titanate $Sm_{0.75}Bi_{3.25}Ti_{3-x}Nb_xO_{12}$ ($x = 0$ and 0.03) polycrystalline samples were prepared by the solid-state reaction route and lattice parameters were calculated from the XRD data. AC-impedance measurements have been carried out in the frequency range of 100 Hz to 1 MHz from RT to 500 °C showing that the samples are non-Debye type. In addition, complex impedance plots along with the detailed ac-conductivity analysis were used to understand the heterogeneity of the electro-ceramics. Results are corroborated with the proposed defect formula and the modified Jonscher's analysis.

Keywords: Electrical ac-conductivity; BLSF; Impedance and modulus spectroscopy; Universal Jonscher's modified law

1. Introduction

Bismuth layered structure ferroelectric (BLSF) materials of Aurivilliu's family have attracted much attention in view of their scientific as well as ferroelectric random access memory (FRAM) application oriented importance [1–4]. The structure of these compounds consists of bismuth oxide layers $(Bi_2O_3)^{2+}$, interleaved with perovskite blocks of $(A_{n-1}B_nO_{3n+1})^{2-}$ along *c*-axis, where site-A represents Bi/Sm ion and site-B represents Ti/Nb, where n is integer ($n = 3$). Generally, ferroelectric materials are classified into two main categories for FRAM applications, namely lead-free materials and lead-based materials (PZT); the former reported to display superior properties replacing PZT system. Park et al. [2] reported that rare earth-modified BLSF material, namely $La_{0.75}Bi_{3.25}Ti_3O_{12}$ (BLT) is a suitable candidate for FRAM devices, but unfortunately the degradation of polarization (fatigue) and shift in coercive field (imprint) properties are found to be limiting points for BLSF materials from the commercialization point of view. Therefore, different rare earth-modified BLSF materials are being prepared in this direction [5,6].

Chen et al. [7] reported that the oxide electrodes can certainly affect the domain characteristic features of FRAM devices interpreting the domain growth mechanism in terms of resistance (R) and capacitance (C) values of both grain and grain boundaries, extracted from complex impedance spectroscopy. In this connection, they have proposed a new fatigue model on the basis of the oxygen vacancy concentration, mobility, and the existing entrapment sites in the materials.

Impedance spectroscopic analysis is a well-known powerful technique to separate out both grain and grain boundary effects present in ferroelectric materials [8–10]. Moreover, the electrical properties are determined by assuming the parallel combination of resistance and capacitance of both grain and grain boundary network. This analysis not only reveals the relaxation mechanism but also gives information about their defect contribution states to the total ac-response under given set of experimental conditions.

Jonscher's Universal power law is being widely used to describe and to interpret the experimental conductivity data of many disordered solids including ferroelectric materials [9]. The global changes of the ferroelectricity, introduced by the different modifications in the compound, can be studied by frequency-dependent ac-conductivity plots. However, ac-conductivity measurement at different frequencies and temperatures σ_{ac} (f, T) is often used to characterize the hopping movement of charge species in the disordered materials like polymers, inorganic glasses, semiconductors, etc. [9].

* Corresponding author.
E-mail addresses: nvp1969@rediffmail.com, nvp1969@yahoo.com (N.V. Prasad).

0272-8842/$34.00
doi:10.1016/j.ceramint.2008.04.019

In view of the afore-mentioned points, a systematic impedance analysis is adopted in the present investigation to understand the effect of cationic role, especially electrical properties, on A-site and B-site samples. Apart from this, the knowledge of ionic relaxation species might give insight on frequency–temperature-dependent impedance along with modulus data for the development of microelectronic devices leading for a detailed study; these results were corroborated with the ac-conductivity data for further understanding.

2. Experimental

New polycrystalline samples of Sm (A-site) and Sm and Nb (A- and B-site)-doped bismuth titanate, namely $Sm_{0.75}Bi_{3.25}Ti_3O_{12}$ (SBT) and $Sm_{0.75}Bi_{3.25}Ti_{2.9625}Nb_{0.03}O_{12}$ (SBNT), were prepared using the solid-state reaction method with reactant powders of AR grade, obtained from Himedia (India), were used in the present analysis. The stoichiometric mixtures of Bi_2O_3, Sm_2O_3, TiO_2 and Nb_2O_5 were finely ground thoroughly, calcined for 4 h, reground and pressed into cylindrical pellets, and were sintered at 1100 °C for 4 h.

The crystal structure of the sample (SBNT) was characterized by XRD pattern, using model PW 3040/60 (x'print) with Cu Kα radiation shown in Fig. 1. Since the radius of the pentavalent Nb^{5+} (0.64 Å) is not significantly different from the Ti^{4+} (0.605 Å) ion, no appreciable change was observed in the SBNT XRD pattern when compared to SBT XRD pattern. The presence of Bi_2O_2 layers might impose such restriction to prevent the possible reduction in lattice parameters. SBNT lattice parameters, calculated on the basis of $Bi_4Ti_3O_{12}$, are as follows: $a = 5.447$ Å, $b = 5.410$ Å, and $c = 32.810$ Å. In the aspect of density, the theoretical and experimental density values eventually state that the present samples are found to be ∼97% of XRD density.

Impedance measurements were measured as a function of frequency (100 Hz to 1 MHz) and the temperature range of 30–500 °C by Solartron low frequency impedance analyzer. The ac-conductivity data was extracted from the impedance data [6,11]. Prior to the electrical measurements, high-temperature silver paste was coated on both sides of the cylindrical pellets and annealed at 500 °C for 30 min.

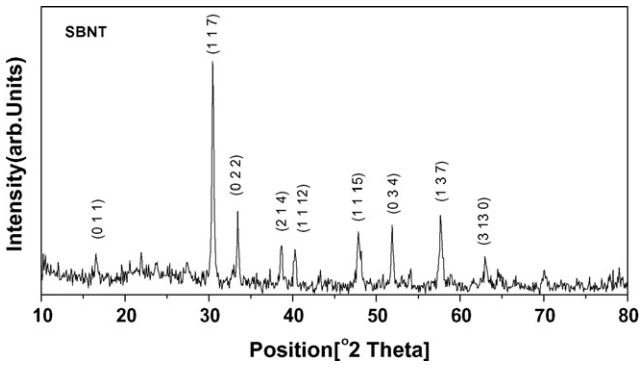

Fig. 1. XRD pattern of SBNT.

3. Results and discussion

Impedance (Z) and modulus (M) spectroscopic plots, shown in Fig. 2(a and d), clearly indicate that the maxima of imaginary components of modulus (M'') are found to shift towards higher frequency domain with increasing temperature. This type of general behavior suggests that the spectral intensity of relaxation times is activated thermally in terms of hopping of charge carriers. Apart from this, a shift in peak position in forward direction indicates that the relaxation time decreases with temperature. A noteworthy aspect is that the full width at half maximum (FWHM) is found to be higher than ideal Debye type (1.16). Moreover the M'' curves are found to be asymmetric in nature and observed that all the Z'' (imaginary part of impedance) curves are found to decrease with increasing temperature and merge with one another at higher frequency scale. This may be due to the release of space charges as a result of reduction in the barrier properties of materials with the rise in temperature and may be responsible factor for the enhancement of ac-conductivity at higher frequencies. The same phenomenon can be correlated to the increasing trend of M'' values, above 100 kHz, in M'' vs. frequency plots.

The distribution of peaks over a frequency domain scale is attributed to the cooperative many body relaxation process and is governed by Universal Jonscher's law. The variation of M''/M''_{max} with f/f_{max} (scaled modulus spectroscopic plot), shown in Fig. 3, gives more plausible information to many body relaxation phenomenon. From the plot, it can be seen that the modulus peaks appear to fall in to a single master curve with slight shift. Such deviation observed in intermediate frequencies (sub-diffusive region) indicates that the relaxations are not completely independent of temperature. These types of relaxation are generally defined as non-Debye relaxations or polydispersive relaxations.

It is known fact that the ferroelectric properties depend largely on the domain structure, the nature of interaction between domain boundaries and the various sorts of defects. Complex impedance measurements give plausible information about defects, domain walls and other varieties of imperfections. Therefore, complex impedance analysis, associated with both grain and grain boundaries, is found to be an alternative tool to study the defect structure of ferroelectric material. Fig. 4(a and b) shows the complex impedance plot for both the samples SBT and SBNT, respectively. The resistance and capacitance of both grain and grain boundary, calculated at 400 °C from the fitting programme, are depicted in the plot. The broad semicircular behavior, associated with grain and grain boundary effects, can be corroborated to ferroelectric domains. From the plots it is clearly observed that B-site-modified sample (SBNT) has broader nature, when compared to A-site-modified sample (SBT). Apart from this, almost equal contribution of both grain and grain boundary for SBNT sample eventually emphasizes the diffuse phase transition (relaxor-like) behavior of the sample due to the competitive interaction of both short-range and long-range orders. More aspect of this mechanism would be discussed in conduction part.

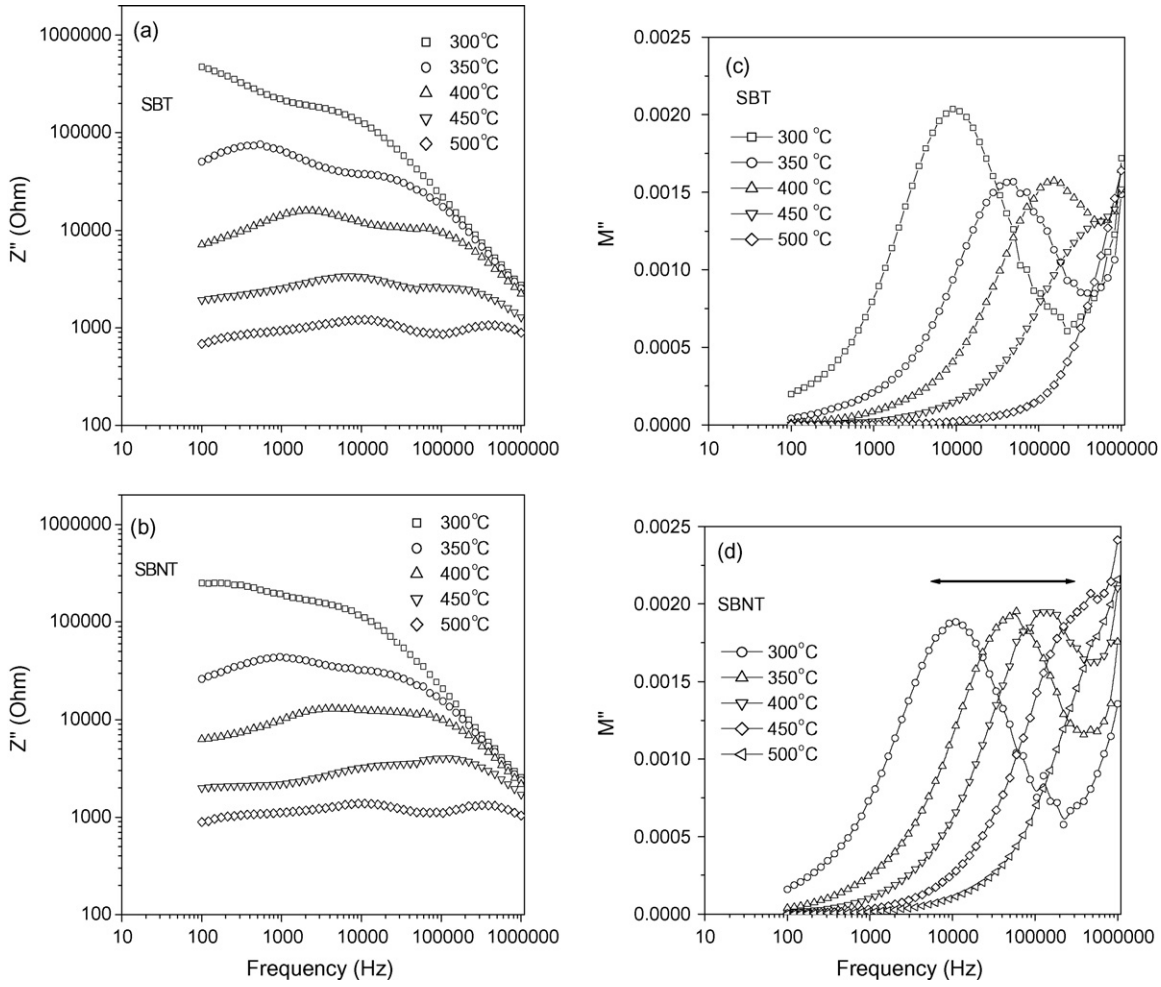

Fig. 2. (a and b) Variation of imaginary part of impedance with frequency. (c and d) Variation of imaginary part of modulus with frequency.

The variation of ac-conductivity with frequency at different temperatures is shown in Fig. 5(a and b). From the plot it is clear that the total conductivity is found to change slowly at lower frequency and at intermediate region it is strongly frequency dependent. However at far high temperatures the conductivity is found to be independent of frequency. Recently Mahesh Kumar and Ye [12] demonstrated such deviations observed in the ferroelectric materials are due to the inhomogeneous nature or migration of anionic and cationic vacancies. They also explained that the modified Universal law ($\sigma\,(f) = \sigma_{dc}[1 + (f/f_p)^n + (f/f_q)^m]$, where f_p and f_q represent lower and higher relaxation frequencies and 'm' and 'n' are exponents) give plausible explanation in lower and higher frequency domain, respectively. Moreover, the temperature-independent and temperature-dependent natures are attributed to the diffusive and sub-diffusive nature of the mobile charges in homogeneous and non-homogeneous potential environments.

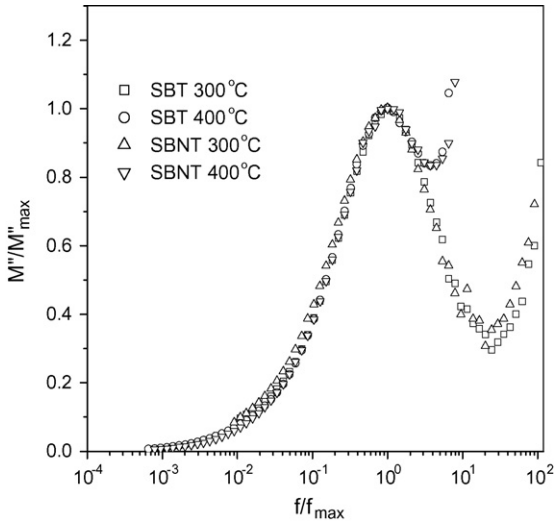

Fig. 3. M''/M''_{max} vs. f/f_{max}.

However, in the present analysis, dc-conductivity data can be theoretically predicted from the extrapolation of ac-conductivity data on y-axis at 1 Hz frequency. The diffusive nature of ac-conductivity at lower temperatures shows single relaxation and multiple relaxations, namely double relaxations, were observed for the data above 200 °C. Relaxation points are indicated by filled circles and squares in the plot (Fig. 5a and b), designated as f_p and f_q, respectively. This indicates that there exist two types of hopping mechanism in the material above 200 °C. Above 400 °C again a single relaxation is observed and

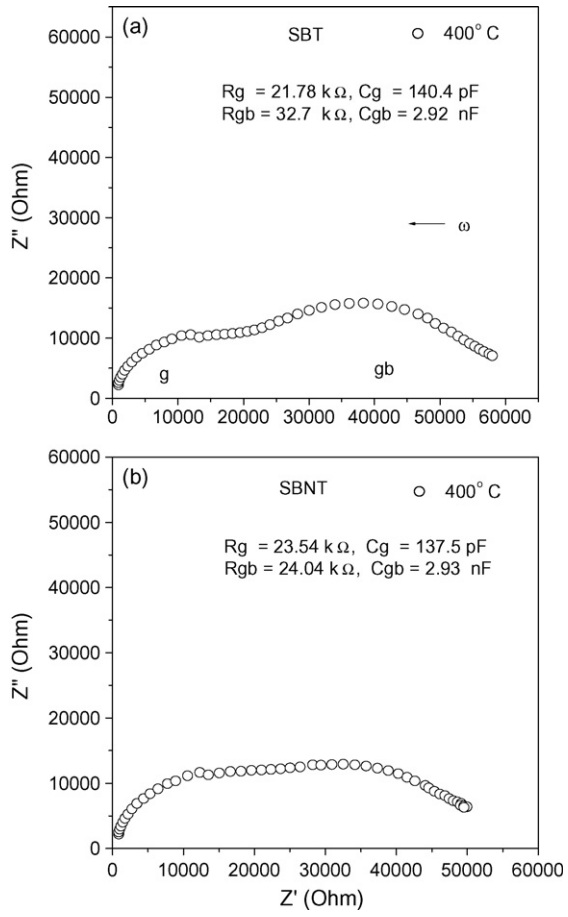

Fig. 4. (a and b) Z'' vs. Z' (Cole–Cole plots for SBT and SBNT at T_c).

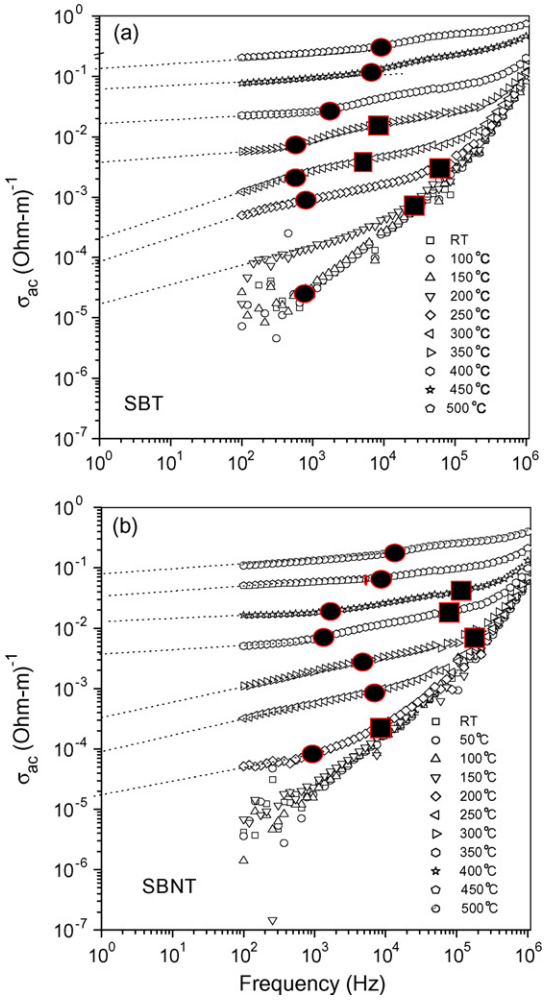

Fig. 5. (a and b) AC-conductivity vs. frequency for SBT and SBNT.

the slope is found to be independent of conductivity. This is due to the very small difference between the two relaxations and f_q dominates over large frequency range starting from very low frequency. However, the different exponent (slope) values found in intermediate temperature regions (200–400 °C) were attributed to the different ionic conduction mechanisms and pathway frequencies.

The variation of dc-conductivity with inverse of temperature (shown in Fig. 6a and b) data exactly fits the Arrhenius behavior and the activation energy values for SBT and SBNT were found to be roughly 1.0 eV and 0.93 eV, respectively. The variation of ω_p with inverse temperature is shown in Fig. 6c. An important observation from the plot (Fig. 6c) is that ω_p is independent of temperature up to certain temperature, namely transition temperature (T_c), and thereafter ω_p becomes temperature-dependent nature. Such temperature-dependent nature of ω_p, for both the samples (above T_c), is attributed to the relaxor-like behavior of the sample. This type of relaxor-like behavior is attributed to the ordering of the defect dipoles. Below the transition temperature short-range polar order predominates more, making ω_p non-Arrhenius behavior. A peak observed near 200 °C in the variation of ω_p with inverse temperature of SBNT (Fig. 6c) data is attributed to the suppression of oxygen vacancy. Similar type of anomalies was observed in Nb-doped $Bi_4Ti_3O_{12}$ ceramics [13]. However, it has been reported in the literature that the cationic vacancies and the intrinsic oxygen vacancies are paired up to form ferroelectric dipoles in BLSF materials and these ferroelectric dipoles are involved not only in hopping-type conduction phenomena but also in relaxor-like nature and the structural transformation, from ferroelectric phase (FE phase) to paraelectric phase (PE phase), of this type materials is mainly attributed to the rearrangement of ions and their defects. Apart from this, BLSF solid solutions lose oxygen traces at elevated temperatures and therefore, during the sintering process, the compensated lattice defects are eliminated by releasing electrons and holes in donor (charge more) and acceptor (charge less) levels [14] and hence, the present solid solutions become non-stoichiometric. The two possible incorporated reactions are given below:

(i) A-site donor dopants SBT (Sm^{3+} doped in place of Bi^{3+}):

$$Bi_2O_3 \rightarrow \tfrac{1}{2}O_2(gas) + V_I + 2e'$$

In the above reaction, V_I is the interstitial vacancy and e' is the singly ionized electron. By substituting Sm^{3+} in place of Bi^{3+} the ionic defects can be compensated by restoring the electrons.

(ii) A- and B-site donor dopants (Sm^{3+} doped for Bi^{3+} site and Nb^{5+} doped for Ti^{4+} site):

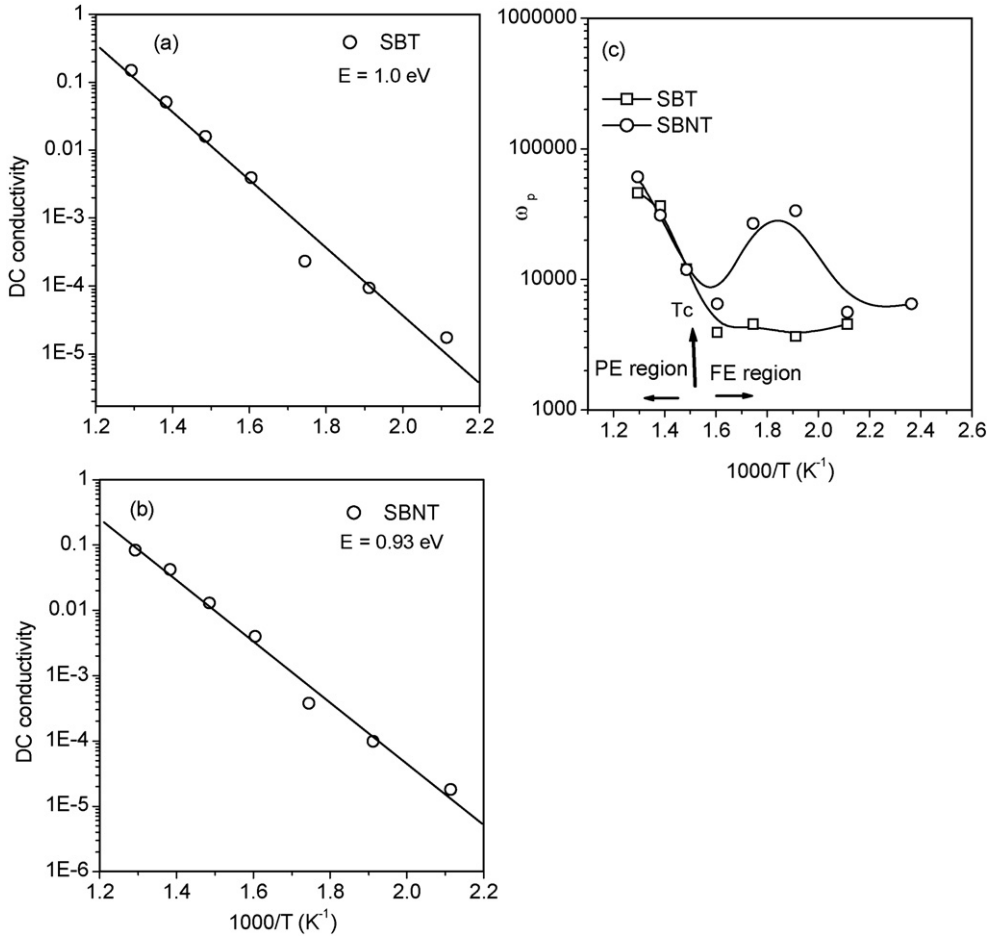

Fig. 6. (a and b) Variation of dc-conductivity with inverse temperature. (c) ω_p vs. inverse of temperature (hopping conductivity frequency–temperature plot).

Under charge neutrality condition, a positive charge centre at Nb site and an electron will be created, by substituting Nb^{5+} in place of Ti^{4+}, described as $Nb_{Ti}^{\bullet} + e'$. These electrons (e') certainly neutralize the influence of holes. These results can certainly be correlated to the conductivity (conductivity (σ) = $nq\mu$, where n is the number of carriers, q is the charge and μ is the mobility) and hence in activation energy values. As mentioned earlier, Nb modification for B-site does not induce any structural changes to the crystal lattice and therefore it is evident that the hole carrier density (n) decreases with Nb modification and moreover Nb doping compensates the oxygen vacancies also ($V_o^{\bullet\bullet} + 1/2\ O_2 \Leftrightarrow O_o + 2h^{\bullet}$, where $V_o^{\bullet\bullet}$ is oxygen vacancy and $h^{\bullet}$ is singly ionized hole). In other words, the holes get trapped in the Nb^{5+}-doped materials (SBNT).

It has been reported by us [6] that the substitution of A- and B-site significantly effects the impedance properties. The broad modulus spectroscopic and complex plots observed in the present investigation are attributed to the random arrangement of cations in the structure, leading to microscopic heterogeneity in the composition. The proposed defect formulas for both the compounds are summarized in Table 1. The bracket term in the formula represents the unoccupied site.

On the basis of the above results one can conclude that the unoccupied sites created by substitution of Sm in place of Bi and intrinsic oxygen vacancies are expected to pair up to form dipoles which involve not only hopping-type conduction phenomena but also relaxor-like behavior in the samples. This tentative conclusion is drawn from the room temperature ac-conductivity vs. frequency plot, where the conductivity is found to be almost frequency-dependent nature (Fig. 5(a and b)). Room temperature exponent (slopes of ac-conductivity vs. frequency plots) values for both the samples (SBT and SBNT) are found to be 0.93 and 0.90, respectively. These values, close to the ideal Jonscher's value (where exponent ∼1), certainly confirm the same phenomenon. More relaxor-like behavior of SBNT is attributed to the competitive interaction of both short-range and long-range orders above and below the transition temperature and braking of the long-range order into short-range order by the rearrangement of ions and their defects. This

Table 1
Proposed defect formula

Compound	Proposed defect formula
A-site-modified compound (SBT)	$Bi_2O_3\ 3(Sm_{0.75/3}Bi_{1.25/3}[]_{1/3}TiO_{4-d})$
A- and B-site-modified compound (SBNT)	$Bi_2O_3 3(Sm_{0.75/3}Bi_{1.25/3}[]_{1/3}$ $Ti_{2.9625/2}Nb_{0.03/2}[]_{0.0075/3}O_{4-d})$

is clearly reflected as peak in hopping conductivity frequency–temperature plot (Fig. 6c).

4. Conclusions

On the basis of the above facts one can conclude that substitution of Sm^{3+} in place of Bi^{3+} creates unoccupied sites, lone pair electrons and oxygen vacancies, which are expected to pair up to form dipoles. From the hopping conduction frequency (ω_p) and inverse temperature plot, it is concluded that hopping of mobile charges in ferroelectric region (FE region) is on account of inhomogeneous random potential environment. In case of paraelectric region (PE region), temperature-dependent ω_p is attributed to the readjustment of defect dipoles and competitive interaction of both short-range and long-range ordering. The transition region, where sudden increase of ω_p (at T_c), is an indicative of competitive interaction of both long-range and short-range ordering and a transition from long-range to short-range ordering. Due to the presence of different types of cations occupying A- and B-site randomly in the lattice and in the formula, leading to relaxor-like behavior in the samples. Creating more uncoupled sites at A- and B-site (shown in Table 1) results SBNT more relaxor-like behavior, compared to SBT. These results are reflected in both spectroscopic as well as complex plots by showing same magnitude of M'' (shown as double arrow in Fig. 2d) and equal grain and grain boundary contributions (Fig. 4b) near transition temperature. Studies are in progress to understand such competitive interactions and its effects in conductivity and other function parameters like hopping frequency (ω_p), hopping distance (R_{min}), etc.

Acknowledgements

One of the authors NVP thanks Department of Science and Technology, New Delhi for sanctioning the SERC-DST Fast track Young Scientist Proposals (SR/FTP/PS-32/2003) and is thankful to the Siddhartha Academy of General & Technical Education, Vijayawada for giving constant encouragement. Authors thank the referee for useful comments while revising the manuscript.

References

[1] E.C. Subba Rao, J. Phys. Chem. Solids 23 (1962) 665.
[2] B.H. Park, B.S. Kang, S.D. Bu, T.W. Noh, J. Lee, W. Jo, Nature 401 (1999) 682.
[3] K. Uchino, Ferroelectric Devices, Marcel Dekker Inc., NY, 2000.
[4] V.K. Wadhawan, Introduction to Ferroic Materials, Gordon & Breach, UK, 2000.
[5] J.L. Pineda Flores, E. Chavira, J.R. Gasga, A.M. Gonzalez, A.H. Tera, J Eur. Ceram. Soc 23 (2003) 839.
[6] N.V. Prasad, S. Karmakar, S.M. Gupta, Int. J. Mod. Phys. B 21 (2007) 1875.
[7] T.C. Chen, C.L. Thio, S.B. Desu, J. Mater. Res. 12 (1997) 2628.
[8] M.E. Lines, A.M. Glass, Principles and Application of Ferroelectric and Related Materials, Clarendon Press, Oxford, 1977.
[9] A.K. Jonscher, Dielectric Relaxation in Solids, Chelsa Dielectric Press Ltd., London, 1983.
[10] D.C. Sinclair, A.R. West, J. Appl. Phys. 66 (1989) 3850 (J. Mater. Sci. 29 (1994) 6061).
[11] M. Chandra Sekhar, N.V. Prasad, Ferroelectrics 345 (2006) 45.
[12] M. Mahesh Kumar, Z.G. Ye, Phys. Rev. B 72 (2005) 024104.
[13] H.S. Shulman, D. Damjanovic, N. Setter, J. Am. Ceram. Soc 83 (2000) 528.
[14] A.J. Moulson, J.M. Herbert, Electroceramics, Chapmann & Hall, London, 1990.